LA-UR- 02-2307

Approved for public release; distribution is unlimited.

Title:

VALIDATION OF THE TRANSIENT STRUCTURAL RESPONSE OF A THREADED ASSEMBLY (U)

Author(s):

Scott W. Doebling, Los Alamos National Laboratory, ESA-WR

François M. Hemez, Los Alamos National Laboratory, ESA-WR

John F. Schultze, Los Alamos National Laboratory, ESA-WR

Submitted to:

4th AIAA Non-deterministic Approaches Forum
Denver, Colorado, April 22-25, 2002

Presented at 4th AIAA Non-Deterministic Approaches Forum
April 22-25, 2002 Denver, Colorado
Approved for Unlimited Release LA-UR-02-2307

AIAA-2002-1644

VALIDATION OF THE TRANSIENT STRUCTURAL RESPONSE OF A THREADED ASSEMBLY

Scott W. Doebling*, Francois M. Hemez†, John F. Schultze‡

Engineering Sciences and Application Division
ESA-WR, Mail Stop P946, Los Alamos National Laboratory
Los Alamos, New Mexico 87544, U.S.A.

ABSTRACT

This paper will demonstrate the application of model validation techniques to a transient structural dynamics problem. The problem of interest is the propagation of an explosive shock through a complex threaded joint that is a surrogate model of a system assembly. The objective is to validate the computational modeling of the key mechanical phenomena in the assembly, so that the component can be represented with adequate fidelity in the system-level model. A set of experiments was conducted on the threaded assembly where the acceleration and strain responses to an explosive load were measured on mass-simulators representing payloads. A significantly detailed computational model of the threaded assembly was also created. Numerical features that represent the important characteristics of the response were defined and calculated for both the experimental and computational data. Each step of the model validation process will be described as applied to this problem. Fundamental issues regarding the nature of model validation and the role of model validation in the engineering analysis process will also be discussed.

I. INTRODUCTION

Model validation refers to the process of assessing the accuracy of a set of predictions from a computational model with respect to experimental measurements over some domain of the simulation input parameters for a particular application. [1] Historically, structural dynamics model validation has focused on the calculation and optimization of metrics between the measured and simulated linear vibration properties of a structure. In this paper, a case study is presented where a complex structural interface is loaded with a transient dynamic impulse. Because of the nature of the structural response, the use of linear vibration response features is not appropriate, and additional features must be explored. Furthermore, the process of model validation for structural dynamics is shown to consist of much more than the extraction of features and the definition of fidelity metrics.

The case study of interest is the propagation of a short-duration (microsecond-scale) impulse across a threaded interface between metallic parts. The system of interest is a connection known as a "manufacturing joint" where two cylindrical parts are connected via a threaded shell part (known as the "mount" in this study). Two mass simulators connected to the mount represent components of the assembly that are to be monitored for shock response. Because of the sensitive nature of the actual structural system, a surrogate assembly is devised to isolate the mechanisms of interest for the scenario. Validation of the response of this threaded assembly under a surrogate loading environment will be used to gain insight into modeling the fundamental mechanisms that influence the response of the actual system. This case study provides an example of how isolation of local phenomena in a surrogate assembly can be used to validate a sub-model of the global structural response. In the opinion of the authors, this type of approach will become more and more common as the cost of experimentation (especially system-level testing) continues to grow at a rate that is disproportional to the growth in cost for computational modeling and analysis.

* Project Leader, ASCI Engineering Analysis, doebling@lanl.gov, Senior Member AIAA
† Technical Staff Member, hemez@lanl.gov, Member AIAA
‡ Technical Staff Member, schultze@lanl.gov, Member AIAA

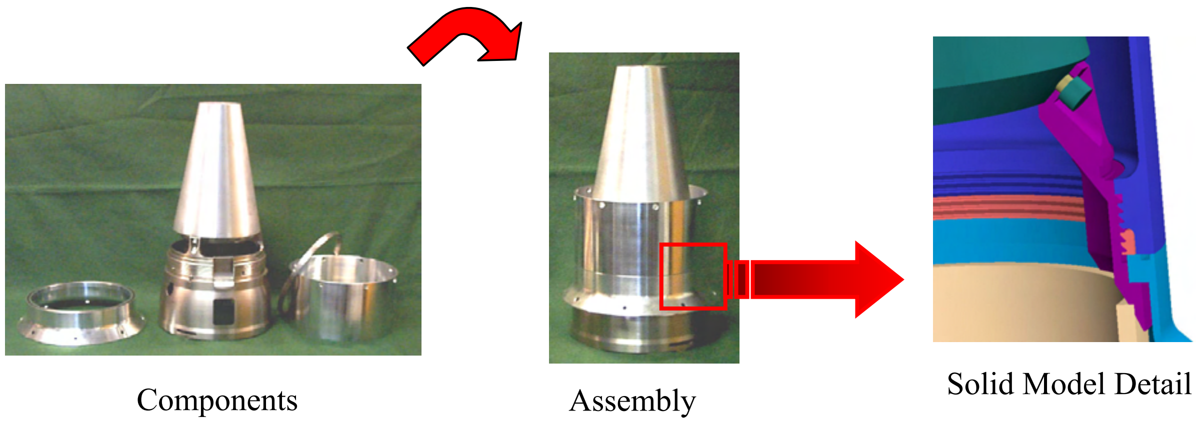

Figure 1: The Threaded Assembly, Components, and Detail of the Manufacturing Joint

This paper provides a summary of the model validation study performed on the threaded assembly. First is a description of the test hardware and the experiments that were conducted. Second is a discussion of the features or characteristics of the response data that are of interest. This is followed by a description of the finite element model used to analyze the response of the assembly, and a discussion of the sensitivity analysis and parameter screening process. Next are brief descriptions of the metamodeling process and the results. Following this section is a description of the test process used to independently measure the friction coefficients between the components. The test/analysis correlation metrics used for the study are next, followed by a discussion of the model revisions and an assessment of the predictive fidelity of the revised model. Finally, some conclusions are presented about the behavior of the assembly and the further work to be conducted.

II. DESCRIPTION OF HARDWARE AND EXPERIMENT

The surrogate assembly is shown in Figure 1, along with a cross-section of the detail surrounding the manufacturing joint. The components consist of the bell-shaped titanium (Ti) "mount"; two aluminum (Al) shells, the "upper shell" that is cylindrical, and the lower shell, that is cylindrical with a "flare" at the bottom edge, and two mass simulators, a conical aluminum mass referred to as the "upper mass simulator" and a cylindrical steel mass referred to as the "lower mass simulator" (not pictured). The upper mass simulator bolts onto the foot-like appendages on top of the mount, and the lower mass simulator is inserted into the bell end of the mount and held in place with a device known as a "tape joint" that essentially consists of two wedges of metal driven into a slot in the mount. Also, a ring-shaped threaded titanium nut is used to hold the lower shell into place on the mount.

The threaded assembly was instrumented with six accelerometers and thirty-three strain gages as shown in Figure 2. The accelerometers provide data on the shock response of the component mass simulators, and the strain gages provide data on the localized propagation of the shock around the circumference of the mount.

The loading was provided by an array of "fingers" of a sheet explosive known as Primasheet 1000 arranged to provide a uniformly distributed impulse, and mounted on a sheet of neoprene to moderate the rise time of the pulse. The test article was suspended vertically for testing via holes in the upper shell. A "light ladder" fiber optic measurement scheme was used to measure the pendulum motion of the test article during the shot, to enable the magnitude of the impulse level to be calculated via an impulse-momentum relationship. Pictures of the suspended test article, the explosive charge, and the light-ladder system are shown in Figure 3. Further details of the experimental configuration may be found in Reference [2].

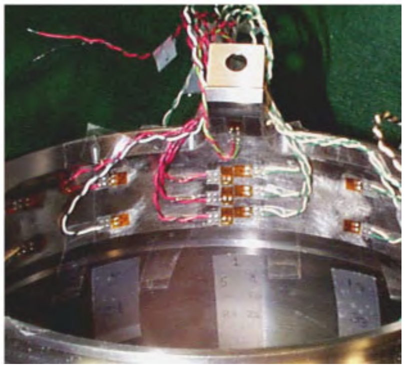

Strain Gages Inside the Mount

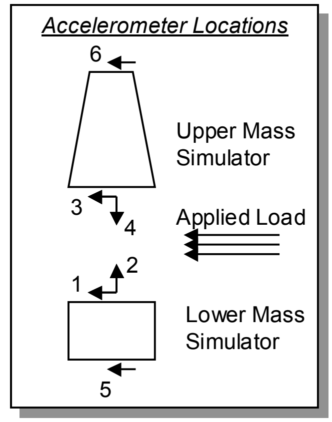

Figure 2: Instrumentation on the Threaded Assembly

Full Test Article

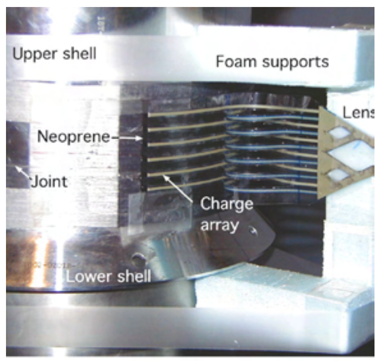

Explosive Charge Array

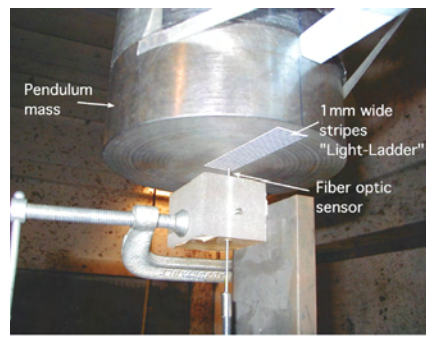

"Light Ladder"

Figure 3: Test Configuration and Explosive Charge Array

A suite of four tests was conducted in July 1999. Two experimental factors were studied in this test suite: The manufacturing tolerance for the Aluminum shells was the first factor. Two different sizes of Al shells were manufactured – one with nominal clearances (the "loose" set) and one with smaller than nominal clearances (the "tight" set). The second factor was an assembly tolerance – specifically, how much radial clearance was allowed between the lower shell and the mount directly behind the location of the explosive charge. The combinations of these factors for each test are shown in Table 1. Tests 1 and 2 were repeated tests intended to give a bound for the test-to-test repeatability. Sample time history and power spectral density (PSD) data for one of the response accelerometers is shown in Figure 4.

Table 1: Test Matrix for the July 1999 Experiments

		Assembly Tolerance	
		Loose	Tight
Manufacturing Tolerance	Loose		Tests 1 & 2
	Tight	Test 3	Test 4

III. FEATURES OF RESPONSE DATA

The data collected from the 4 experiments were compared to each other in an attempt to diagnose the effects of each experimental factor. However, merely overlaying the time history and PSD information as shown in Figure 5 does not give a very clear indication of agreement or disagreement between the data sets. Thus, it was desired to find a characteristics or "features" of the data that, when compared, would indicate whether the signals were in agreement or not. In the realm of linear vibration, modal properties are most often used in this role. However, it is clear from these results that with only 10ms of data, the frequency increment of 100 Hz makes it difficult to accurately identify modal frequencies.

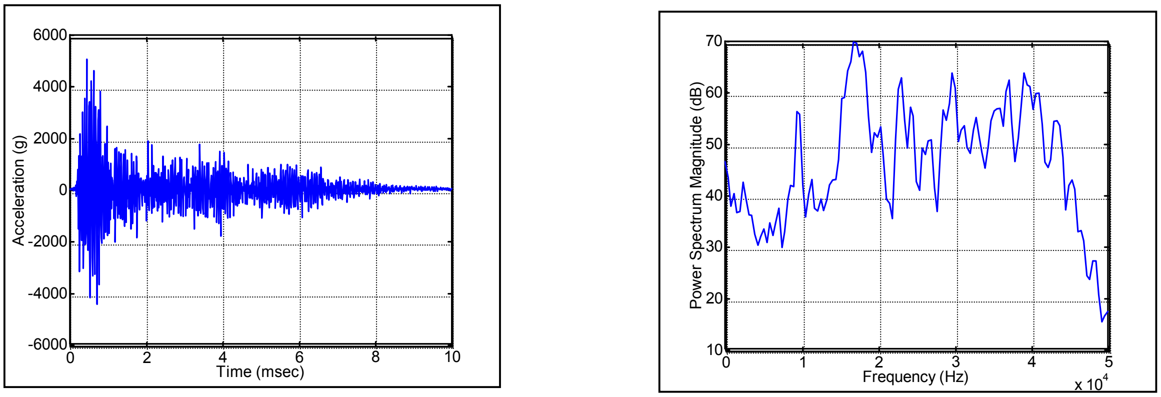

Time History Response

Power Spectral Density

Figure 4: Sample Data from the LANL Threaded Assembly

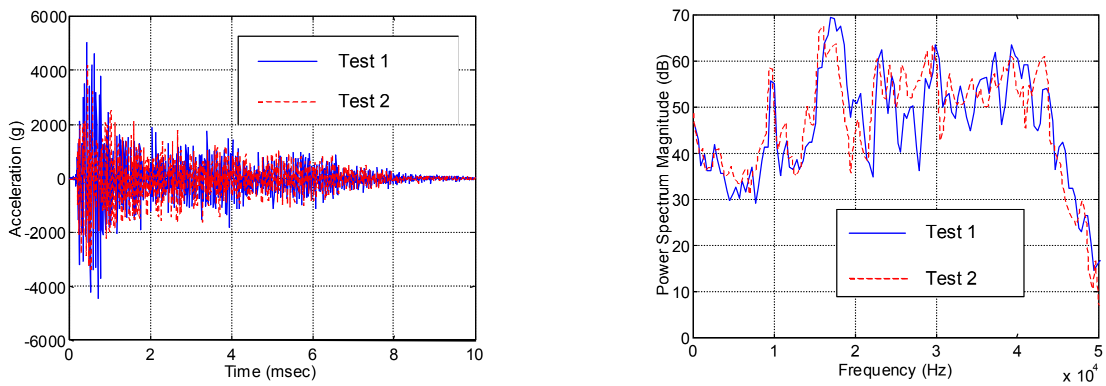

Time History Response

Power Spectral Density

Figure 5: Overlays of Data from Tests 1 & 2

Given the difficulty of identifying the response of this system with conventional modal response features, it seems appropriate to explore what sort of features are commonly used in the analysis of transient shock response. A NASA standard on pyroshock (explosive) testing [3] lists four primary types of features:

- Peak acceleration response
- 10% signal duration or decay time
- Shock response spectrum (SRS)
- Temporal moments

Upon investigation of these 4 types of features, the following determinations were made. The analysts involved with the FE modeling felt that for this type of highly oscillatory response, the peak acceleration and 10% signal duration were not appropriate because there were still many things that could be inaccurate in the signal response. The shock response spectrum, while informational, is still very high dimensional and thus present difficulties in making a comparison between two values. Thus the temporal moments were selected as the features of interest for this analysis.

The temporal moments are scalar-valued features of the time history that are roughly analogous to the statistical moments of a signal. They are able to capture different characteristics of the time signal that can then be compared on a one-to-one basis between different tests, or between test and analysis. The temporal moments are described in more detail in Reference [4] and a special case known as the "central moments" are computed using the following formula:

$$\mathbf{M_i} = \int_{-\infty}^{+\infty} \mathbf{t^i \left(y(t)\right)^2 dt} \qquad (1)$$

From the temporal moments, features can be computed that have physically intuitive meanings about the

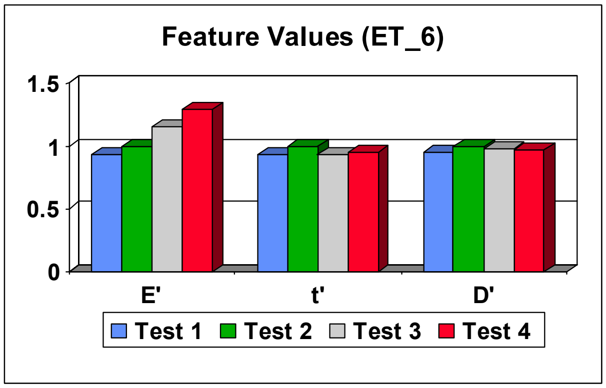

Figure 6: Comparison of Temporal Moments for July 1999 Test Series

content of the signal. The first three such quantities are labeled *E* (energy of the signal), τ (central time, or time at which the signal energy is equal before and after, roughly analogous to the statistical mean), and *D* (root mean square duration, a measure of the dispersion of the signal about the central time, roughly analogous to statistical standard deviation).

The comparison of these first three temporal moment-based features for the 4 tests in the July 1999 test suite is shown in Figure 6. Comparing tests 1 & 2 shows the effect of test-to-test repeatability. Comparing tests 3 & 4 isolates the effects of assembly tolerance and comparing test 4 to tests 1 & 2 isolates the effects of manufacturing tolerance. It would seem from inspection of Figure 6 that manufacturing tolerance has a significant effect and assembly tolerance does not, but it is difficult to decide conclusively without better information on the test-to-test repeatability. After all, only 2 repeatability data points is too few to even compute a standard deviation!

IV. FINITE ELEMENT MODEL OF THE ASSEMBLY

A finite element model was created of the assembly in ParaDYN (the parallel version of DYNA3D) to run on the LANL supercomputer *Blue Mountain*. This model contains an extremely detailed model of the threaded connection between the mount, the shells, and the nut, as shown in Figure 7. This level of detail was required to capture the localized interaction between the parts at the threaded connection. The structure is not axially symmetric, so a 3D finite element mesh is required to adequately represent the dynamic response. The model consists of 1.4 million elements (both solids and shells) and 1.8 million nodes (about 6 million degrees of freedom). Contact is defined between the parts with Coulomb friction. The contact is partitioned into 480 separate pairs to allow the model to be solved in parallel. This model runs on 504 processors on Blue Mountain and takes roughly 1 hour per millisecond of simulation time. For the runs used in this validation study, typically 3ms of simulation time is required. The displacement contours of a typical simulation are also shown in Figure 7.

V. SENSITIVITY ANALYSIS AND PARAMETER SCREENING

The next step in the validation process is sensitivity analysis. The objective of sensitivity analysis is to determine which parameters in the computational model exhibit the most influence on the response features of interest. A first step in sensitivity analysis is the removal of those parameters that are shown to exhibit little or no influence on the response features. This can be accomplished using parameter effects analysis, which is part of the technology known as design of experiments (DoE) [5].

The parameter screening process begins with a list of parameters that the analysts believe are potentially

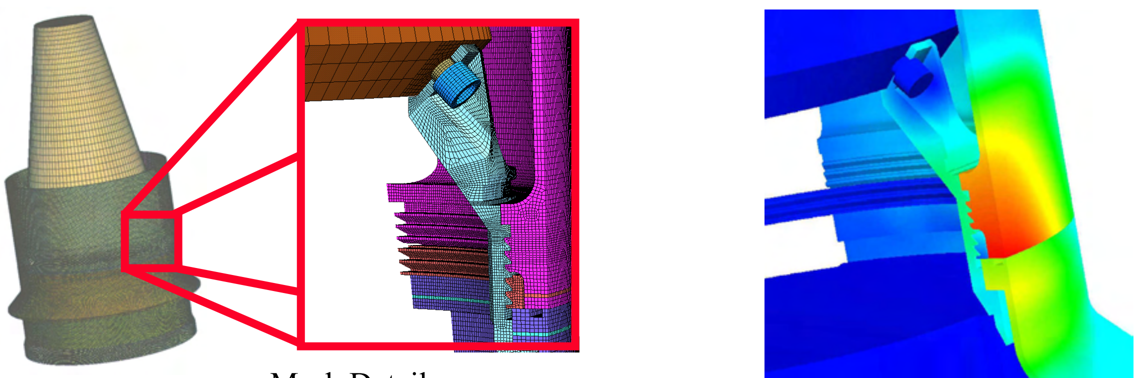

Mesh Detail

Displacement Contours

Figure 7: The Finite Element Model Detail and Typical Displacement Contours

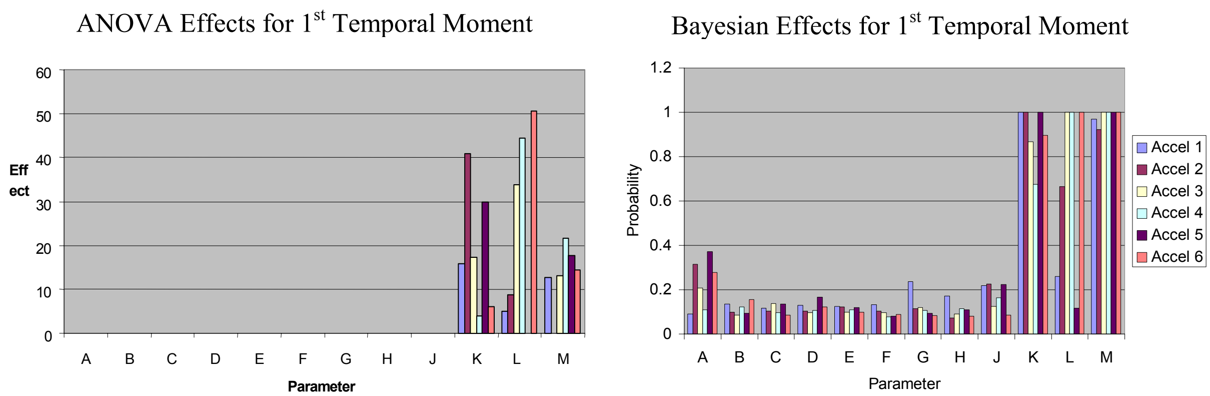

Figure 8: Parameter Screening Results for the Threaded Assembly

influential on the response features. For the threaded assembly, there are a total of 12 parameters on the initial list. These parameters are shown, along with their abbreviation codes, in Table 2.

Assuming 2 values for each of these parameters (i.e. a high and low value), there are a total of 4096 combinations of parameter values from the 12-parameter set. Using a Taguchi orthogonal array criterion [5], 76 of these parameter combinations are selected for simulation runs. The results of these 76 runs are analyzed to perform a parameter effects analysis with sample results from two of the analysis methods shown in Figure 8. Details of these methods can be found in Reference [6]. Figure 8 shows that the parameter screening results obtained with an analysis of variance (ANOVA) technique and a Bayesian screening technique are consistent. In both cases, large vertical bars identify the input parameters responsible for the variability of temporal moment features over the entire design space. From examination of these runs over a number of features for the various accelerometers, the parameter set is screened down to six parameters, shown in Table 3, which are then re-coded as A thru F.

VI. METAMODELING

With the parameter space reduced to dimension six, it is now tractable to compute a metamodel of the FE simulation. A metamodel (a.k.a. response surface model, surrogate model, fast-running model) is simply an alternative model that is used in place of the computational FE model for studying the response of the simulation over the parameter domain. The advantage of using a metamodel is that it can run more quickly than the full FE model, the response surface can be visualized graphically, and it can be made smooth (with proper choice of form) to facilitate optimization.

Table 2: Parameters for Sensitivity Analysis

Parameter Code	Parameter Name
A	Preload – Tape Joint
B	Preload – Retaining Nut
C	Preload – Upper Shell
D	Static Friction – Al/Al
E	Static Friction – Ti/Ti
F	Static Friction – Al/Ti
G	Static Friction – Steel/Ti
H	Kinetic Friction – Al/Al
J	Kinetic Friction – Ti/Ti
K	Kinetic Friction – Al/Ti
L	Kinetic Friction – Steel/Ti
M	Magnitude of Applied Impulse

Table 3: Post-Screening Parameter Set

Parameter Code	Parameter Name
A	Preload – Tape Joint
B	Static Friction – Steel/Ti
C	Kinetic Friction – Al/Al
D	Kinetic Friction – Al/Ti
E	Kinetic Friction – Steel/Ti
F	Magnitude of Applied Impulse

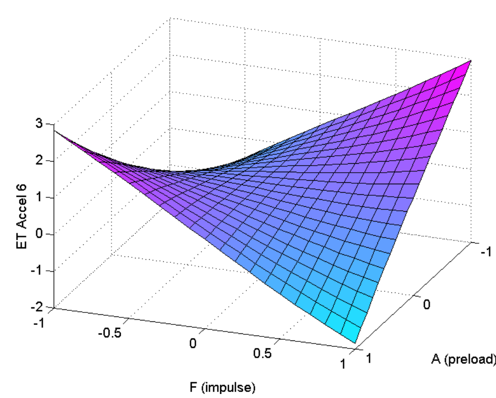

Figure 9: Sample Metamodel Surface for First Temporal Moment of Accel #6 Time History vs. Joint Preload and Impulse Magnitude

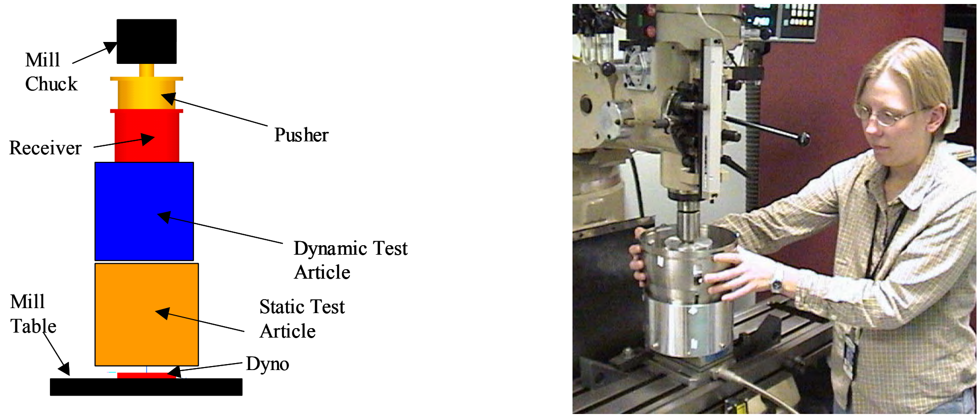

Figure 10: Diagram and Photograph of Friction Coefficient Measurement Rig

For the threaded assembly, an additional set of 64 Taguchi orthogonal array runs are executed, and fit to a 6-parameter cubic polynomial metamodel using a commercial software package. [7] A separate polynomial is fit over all six parameters for each response feature. The resulting metamodel can be visualized for one feature at a time with respect to 2 parameters as shown in Figure 9. The parameters are encoded to the range [-1,1].

VII. MEASUREMENT OF FRICTION COEFFICIENTS

Because four of the six parameters in the reduced parameter set are friction coefficients, an independent set of experiments was conducted to identify the friction coefficients between several of the parts. A fixture was designed to apply an axial load between the parts, and then the resisting torque of the parts is measured as they are rotated with respect to each other. A strain gage dynamometer was used to measure the six-axis forces and moments. A diagram of the assembly and a photograph of the actual experiment are shown in Figure 10. The "dynamic" part is rotated with respect to the "static" part by hand. The parts were tested at two different axial load values, and were tested in the clockwise and counterclockwise directions. Some of the friction coefficients exhibited dependencies on load and/or direction, and it is planned that metamodels will be fit to the friction coefficients to account for these dependencies. Mean estimates of the friction coefficients assuming that these dependencies are negligible appear in Table 4.

Table 4: Mean Estimates of Kinetic Friction Coefficients for Threaded Assembly

Interface	Mean Kinetic Friction Coefficient
Ti-Ti Thread (Lower)	0.6785 ± 0.01160
Ti-Ti Thread (Upper)	0.7156 ± 0.02289
Steel-Ti Edge	0.4379 ± 0.007843
Al-Ti Edge	0.4664 ± 0.007319
Al-Ti Thread	0.7664 ± 0.02421
Al-Al Edge	0.5186 ± 0.01677

VIII. TEST/ANALYSIS CORRELATION METRICS

To assess the fidelity of the computational predictions with respect to the experimental measurements, an appropriate test/analysis correlation metric must be defined. For low-dimensional deterministic features, a typical test-analysis error metric is the error norm between the feature values

$$J_i = \left\| f_i - \hat{f}_i \right\| \qquad (2)$$

In this equation, f_i is the i^{th} measured feature value, $\hat{f}_i$ is the computed feature value, and J_i is the error metric.

In the case of the threaded assembly, there are four measurements of each feature value (one from each experiment). Each experiment also has an independently measured value of applied impulse as measured using the "light ladder" technique described above. Starting with the metamodel surface shown in Figure 9, the measured feature values can be superimposed into the same space. The result is the plot shown in Figure 11. The stars are the four experimental measurements, plotted at their measured values of ET_6 against measured values of F (Impulse magnitude) and A (tape preload). As the tape preload was not measured and is unknown for these tests, it is assigned a value at the mean (A=0).

The error metric is then defined as the distance from each experimental point to the surface. While this might be done using the minimum distance to the

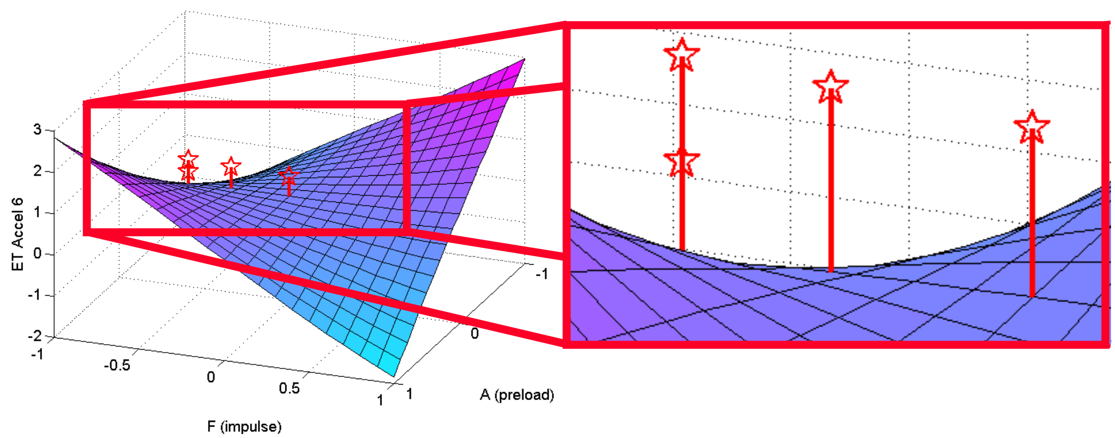

Figure 11: Test-Analysis Correlation Using a Metamodel for the LANL Threaded Assembly

surface as shown in Equation 3, for this study it is defined as the distance in the vertical (feature) direction at the estimated location of the experiment in the parameter space, $\widetilde{P}_i^k$ for the i^{th} feature of the k^{th} experiment, as shown in Equation 4. Using the definition in Equation 4, and taking the norm over all four experimental points, yields an overall TAC metric for this feature shown in Equation 5.

$$J_i = \min_p \left(\left\| f_i - \hat{S}(p) \right\| \right) \quad (3)$$

$$J_i = \left(\left\| f_i - \hat{S}\left(\widetilde{P}_i^k\right) \right\| \right) \quad (4)$$

$$J = 0.9337 \quad (5)$$

IX. MODEL REVISION AND ASSESSMENT OF PREDICTIVE ACCURACY

Upon examination of the test/analysis correlation metric shown in Section VIII, revisions can be brought to the model in an attempt to improve the fidelity of the model prediction. The first improvement is the use of the measured friction coefficients shown in Table 4 as an alternative to assumed friction coefficient "handbook value" used in the initial evaluation of the metamodel surface shown in Figure 9. Simply substituting the new values of friction coefficient into the metamodel and repeating the test/analysis correlation analysis from Section VIII yields the new comparison shown in Figure 12. Inspection of Figure 12 relative to Figure 11 indicates that the experimental points are now much closer to the metamodel surface. Evaluation of the metric of Equation 4 yields the error

$$J = 0.3940 \quad (6)$$

metric magnitude shown in Equation 6, which is significantly reduced from the original value shown in Equation 5. Thus, using the new friction coefficients in the metamodel significantly improves the value of the test/analysis error metric.

Another revision that can be brought to the computational model is the separation of the contact model of Aluminum vs. Titanium into two different contact types, one where they meet edge-on-edge, and one where they meet thread-on-thread. It is apparent from Table 4 that these two interface types have significantly different friction coefficients. This type of model revision may then be sufficient motivation to rerun the original computational model and re-compute the metamodel used in the test/analysis correlation analysis.

Only one parameter is left with significant uncertainty

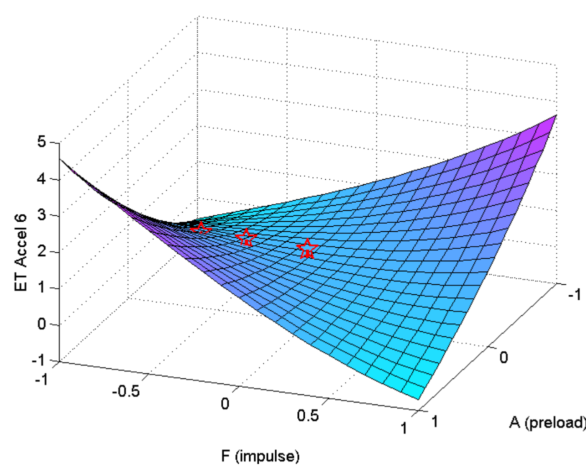

Figure 12: Improved Test-Analysis Correlation for the LANL Threaded Assembly Using Measured Values for Friction Coefficients

surrounding it: the preload of the tape joint. One approach to compute this parameter is to use optimization techniques to calibrate values of this parameter with respect to each experimental measurement. The resulting preloads can then be entered into the computational model. If this path is chosen, however, care should be taken to make an independent assessment of the predictive accuracy. In other words, the metric used to assess predictive accuracy of the model must be independent of the metrics used to calibrate the values. This issue points to the general need in the structural dynamics community for a method to preserve the independence of calibration and validation results by partitioning the available data, as is commonly done in the neural network community. [8]

X. CONCLUSIONS

This paper has presented a case study of model validation technology applied to the isolation, modeling, and validation of complex mechanical phenomena in structural dynamics. The approach described is sufficiently general as to be applicable to a wide range of problems in structural dynamics. Specifically addressed are the issues of conceptual modeling, definition of appropriate response data features, sensitivity analysis and parameter screening, metamodeling, the independent assessment of key parameters, definition of appropriate test/analysis correlation metrics, application of model revisions, and the assessment of model predictive accuracy. Not covered in this analysis, but also important, is the analysis of computational and experimental uncertainties. Future work will include more experimentation to assess experimental uncertainties and further explore the parameter space, and more formal assessment of the model predictive accuracy.

XI. ACKNOWLEDGMENTS

Various Los Alamos National Laboratory programs supported this work. The pyroshock testing was designed and performed by SRI International of Menlo Park, California, who also provided the photos of the experimental apparatus. The authors wish to express significant recognition to LANL staff Tom Butler, Amy Robertson, and Jason Pepin, SRI staff Mark Groethe, and LANL graduate students Amanda Cundy (Virginia Tech University) and Jeff Hylok (University of Cincinnati).

XII. REFERENCES

[1] Doebling, S.W., Hemez, F.M., Schultze, J.F., and Girrens, S.P., "Overview Of Structural Dynamics Model Validation Activities At Los Alamos National Laboratory," *Proc. 4th AIAA Non-Deterministic Approaches Forum*, Denver, Colorado, April 2002. AIAA-2002-1643.

[2] Groethe, M., "Manufacturing Joint Validation Tests," Final Technical Report, SRI Project 10129, November 1999.

[3] Mulville, D.R., "Pyroshock Test Criteria," NASA Technical Standard, Report NASA-STD-7003, May 1999, http://standards.nasa.gov.

[4] Smallwood, D.O., "Characterization and Simulation of Transient Vibrations Using Band Limited Moments," *Shock and Vibration*, Vol. 1, No. 6, 1994, pp. 507-527.

[5] Myers, R.H. & Montgomery, D.C., 1995, *Response Surface Methodology: Process and Product Optimization Using Designed Experiments*, Wiley Interscience, New York.

[6] Cundy, A.L., Schultze, J.F., Hemez, F.M., Doebling, S.W., and Bingham, D., "Variable Screening In Metamodel Design For A Large Structural Dynamics Simulation," *Proc. IMAC XX*, Los Angeles, California, Feb 2002.

[7] *Design Expert Version 6 User's Guide*, Stat-Ease, Inc. 2000, http://www.stat-ease.com

[8] Bishop, C.M., 1995, *Neural Networks for Pattern Recognition*, Oxford University Press, New York.